Effect of emitter layer doping concentration on the performance of a silicon thin film heterojunction solar cell*

Zhang Lei(张 磊)[a], Shen Hong-Lie(沈鸿烈)[a)b)†], Yue Zhi-Hao(岳之浩)[a], Jiang Feng(江 丰)[a], Wu Tian-Ru(吴天如)[a], and Pan Yuan-Yuan(潘园园)[a]

[a] College of Materials Science and Technology, Nanjing University of Aeronautics and Astronautics, Nanjing 210016, China
[b] Key Laboratory for Intelligent Nano Materials and Devices of the Ministry of Education Nanjing University of Aeronautics and Astronautics, Nanjing 210016, China

(Received 15 May 2012; revised manuscript received 11 June 2012)

A novel type of n/i/i/p heterojunction solar cell with a-Si:H(15 nm)/a-Si:H(10 nm)/ epitaxial c-Si(47 μm)/epitaxial c-Si(3 μm) structure is fabricated by using the layer transfer technique, and the emitter layer is deposited by hot wire chemical vapour deposition. The effect of the doping concentration of the emitter layer S_d (S_d=PH_3/(PH_3+SiH_4+H_2)) on the performance of the solar cell is studied by means of current density–voltage and external quantum efficiency. The results show that the conversion efficiency of the solar cell first increases to a maximum value and then decreases with S_d increasing from 0.1% to 0.4%. The best performance of the solar cell is obtained at $S_d = 0.2\%$ with an open circuit voltage of 534 mV, a short circuit current density of 23.35 mA/cm^2, a fill factor of 63.3%, and a conversion efficiency of 7.9%.

Keywords: layer transfer, silicon thin film heterojunction solar cell, hot wire chemical vapor deposition, doping concentration

PACS: 68.55.aj, 81.15.Gh, 88.40.jj **DOI:** 10.1088/1674-1056/22/1/016803

1. Introduction

The photovoltaic industry urgently needs to reduce silicon material consumption. From this point of view, many efforts have been made to fabricate silicon thin film solar cells.[1–4] Obtaining high-quality silicon films is the key to fabricating cost-effective solar cells. The layer transfer technique is a promising approach to fabricating low-cost and high-efficiency solar cells. It can prepare epitaxial silicon thin films with excellent crystalline quality, and the silicon wafer used as the substrate for epitaxial growth can be reused several times.[5,6] In contrast, the c-Si wafer used in traditional solar cell production can be used only once. Phosphorous diffusion is a widely used method for the emitter layer formation of crystalline silicon solar cells, which normally needs a temperature higher than 800 °C.[7,8] To further reduce the energy consumption in the solar cell fabrication process, emitter layers prepared at low temperature show potential. a-Si:H/c-Si heterojunctions are particularly promising, in which an a-Si:H layer is deposited on c-Si.[9] For this structure, plasma-enhanced chemical vapour deposition (PECVD) is normally used for the deposition of a-Si:H.[10,11] However, hot-wire chemical vapour deposition (HWCVD), as a new and promising technique, is more suitable for a-Si:H deposition for its high deposition rate, high gas utilization efficiency, and no ion bombardment.[12–14] However, no one has reported the fabrication of a silicon thin film heterojunction solar cell that comprises a silicon epitaxial layer prepared by the layer transfer technique and a-Si:H emitter layers prepared by HWCVD. Such a solar cell is studied in the present paper.

For the structure, the silicon epitaxial layer is prepared by the layer transfer technique, which involves the formation of double-layer porous silicon (DLPS, composed of a low porous top layer and a buried high porous layer)[15] by the electrochemical etch of a highly doped Si (100) wafer and the epitaxial growth of p-type and intrinsic silicon layers by low pressure chemical vapour deposition (LPCVD). HWCVD is employed to deposit the intrinsic a-Si:H layer and the n-type a-Si:H emitter layers with different doping concentrations for the formation of the junction. The effect of different emitter layer doping concentrations on the performance of the solar cell is studied.

2. Experiments

The DLPS on the surface of highly doped p-type (100)-oriented Czochralski (CZ) silicon wafer (1.5 cm×1.5 cm) was prepared by electrochemical anodization. The top layer had a porosity of 20%, and the buried layer had a porosity of 50%. After the formation of DLPS, an annealing process was carried out at 1100 °C for 30 min in hydrogen atmosphere to restructure the porous silicon layer. In this process, the upper low porous layer recrystallized and formed a so-called quasi monocrystalline silicon (QMS) layer, which acted as the

*Project supported by the National High Technology Research and Development Program of China (Grant No. 2006AA03Z219), the Jiangsu Innovation Program for Graduate Education, China (Grant No. CXZZ11_0206), and the Priority Academic Program Development of Jiangsu Higher Education Institutions, China.

†Corresponding author. E-mail: hlshen@nuaa.edu.cn

© 2013 Chinese Physical Society and IOP Publishing Ltd

template for the following epitaxial growth. The buried high porous layer yielded large cavities and thus transformed into a mechanically weak layer which served as the separation layer. After the annealing process, the epitaxial growths of a p-type layer from SiH_4+B_2H_6 and an intrinsic layer from SiH_4 were carried out with LPCVD at a temperature of 1100 °C and a pressure of 100 Pa. The thicknesses of the p-type and the intrinsic layers were 3 μm and 47 μm, respectively. A detailed description of the above steps can be found in our previous work.[16]

After the growth of the epitaxial layers, the wafer was transferred into a single-chamber HWCVD system immediately. Two tantalum wires with an average diameter of 0.5 mm were used as the catalyzer, and the distance between the tantalum wires and the substrate was 4 cm. First, the chamber was pumped down to a base pressure of about 2×10^{-4} Pa, and then the epitaxial c-Si surface was exposed to 40 sccm hydrogen dissociated by the hot wires heated at 1800 °C for 60 s. After that, a thin intrinsic a-Si:H layer (10 nm) was deposited as the passivating layer, and a series of n-type a-Si:H films (15 nm) with different doping concentrations was deposited as the emitter layers. The doping precursor (PH_3 for n-type a-Si:H) concentration (S_d=PH_3/(PH_3+SiH_4+H_2)) was varied from 0.1% to 0.4%. The deposition parameters of the a-Si:H films are listed in Table 1. In order to characterize the properties of a-Si:H films, intrinsic a-Si:H films, and n-type a-Si:H films, each of them with a thickness of 400 nm was also deposited on the glass substrate.

Table 1. Deposition conditions for a-Si:H emitters of the thin-film heterojunction solar cell.

Type	T_s/°C	H_2/sccm	SiH_4 /sccm	PH_3/sccm	Pressure/Pa
(i) a-Si:H	200	9	4	–	1
(n) a-Si:H	200	12–0	4	4–16	1

As the anti-reflective coating and front conductive layer, an indium tin oxide (ITO) film with a thickness of 120 nm was deposited by radio-frequency (RF) magnetron-sputtering. After the formation of the silver front contact using photolithography, the solar cell was attached to a glass slide by glue. Then the upper film part (solar cell) was separated from the wafer at the buried high porous layer mechanically. The lower silicon part was cleaned and reused. Meanwhile, a mixture of hydrofluoric acid (HF, 40 wt.%) and perhydrol (H_2O_2, 30 wt.%) in a volumetric proportion of 3:1 was used to etch off the residual porous layer on the back side of the cell. ITO+Ag back contacts with thicknesses of 120 nm and 500 nm were deposited by RF magnetron-sputtering respectively. The fabrication process and the structure of the solar cells are shown in Fig. 1.

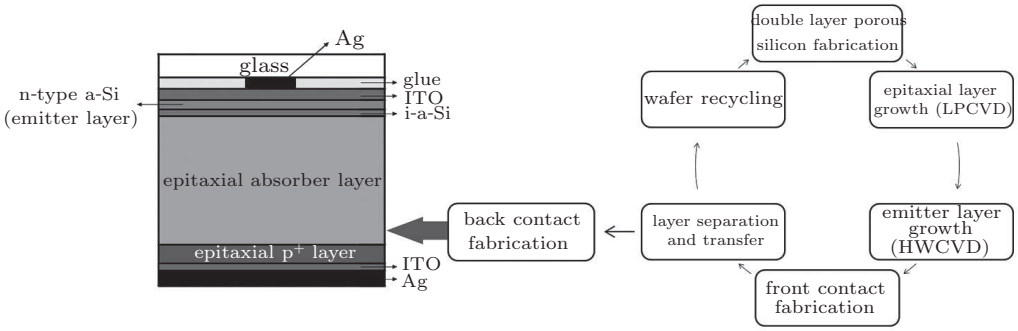


Fig. 1. Fabrication process and schematic diagram of the silicon thin film heterojunction solar cell.

Raman measurements of the epitaxial Si layers and the intrinsic a-Si:H layers were carried out by using JY-T64000 with an excitation wavelength of $\lambda = 514$ nm. The minority carrier life time was characterized by WT2000 (Semilab). The absorption coefficients of the emitter layers with different doping concentrations were recorded in a wavelength range of 300–1200 nm using a Varian Cary5000 spectrophotometer, and the temperature-dependent conductivity of these n-type a-Si:H films was measured by using a Keithley2400 digital sourcemeter. The current density–voltage (J–V) characteristic of the solar cells was measured at 100 mW/cm^2 (AM 1.5) using a solar simulator, and the external quantum efficiency (EQE) was measured in the wavelength range from 300 nm to 1200 nm.

3. Results and discussion

Figure 2 shows the Raman spectra of the monocrystalline silicon wafer and the epitaxial layer. The peak positions and the full widths at half maximum (FWHMs) of the two spectra are almost the same, indicating that the epitaxial absorber layer is perfectly crystallized. The excellent crystalline quality of the absorber layer will guarantee the high efficiency of the silicon thin film heterojunction solar cell. Figure 2 also shows the Raman spectra of the intrinsic a-Si:H. It is shown that the layer is entirely amorphous. The extremely thin in-

trinsic a-Si:H layer acts as a passivating layer to reduce the carrier recombination velocity at the interface.[17–20] The measurement results show that the minority carrier lifetime of the epitaxial layer passivated by the intrinsic a-Si:H layer is about 75 μs, which indicates the effective passivating effect.

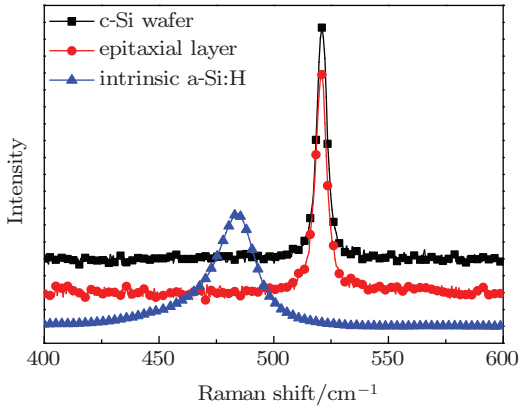


Fig. 2. (color online) Raman spectra of the crystalline silicon wafer, epitaxial silicon films deposited by LPCVD, and a-Si:H deposited by HWCVD.

As described in Ref. [21], the doping concentration of the emitter layer will affect the performance of an a-Si:H (n)/c-Si(p) heterojunction solar cell obviously. So, the effect of doping concentration of the emitter layer on the performance of the silicon thin film heterojunction solar cell is also studied here. Figure 3 shows the *J*–*V* curves of the silicon thin film heterojunction solar cells with different emitter layer doping concentrations. The results are summarized in Table 2. The results show that the most favorable doping concentration for the emitter layer is $S_d = 0.2\%$, under this circumstance the conversion efficiency of the solar cell reaches 7.9%. At a lower doping concentration ($S_d = 0.1\%$), the open circuit voltage (V_{oc}) somewhat decreases, and the short circuit current density (J_{sc}) and the fill factor (FF) noticeably deteriorate. On the other hand, at a higher doping concentration ($S_d = 0.4\%$), a higher V_{oc} is obtained, but J_{sc} is the lowest, the FF dose not descend compared with that of the best solar cell.

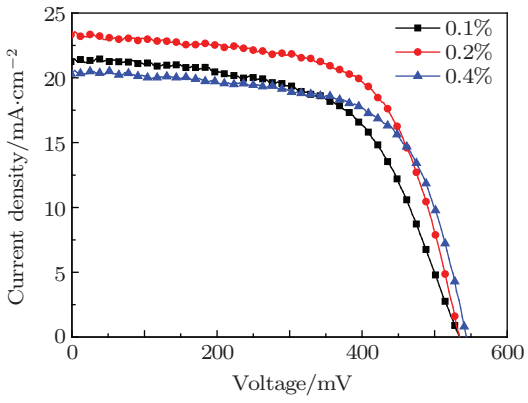


Fig. 3. (color online) Current densities versus voltage for silicon thin film heterojunction solar cells with different emitter layer doping concentrations.

Table 2. Activation energies of the emitter layer and the *J*–*V* test results of the silicon thin film heterojunction solar cells with different emitter layer doping concentrations.

S_d /%	E_a/eV	V_{oc}/mV	J_{sc}/mA·cm^{-2}	FF/%	η /%
0.1	0.54	532	21.45	58	6.62
0.2	0.46	534	23.35	63.3	7.9
0.4	0.34	543	20.46	64	7.12

Figure 4(a) gives the temperature-dependent conductivities of the n-type a-Si:H films with different doping concentrations.

The results are based on the Arrhenius relationship[22] viz.

$$\ln\sigma = -\frac{E_a}{1000k}\frac{1000}{T} + \ln\sigma_0, \tag{1}$$

where σ_0 is the conductivity factor, k is the Boltzmann's constant, and E_a is the conductivity activation energy. The conductivity activation energy E_a of each layer can be obtained from the slope of the corresponding curve in Fig. 4(a). From this figure, we can see that the conductivity increases gradually as the doping concentration increases from 0.1% to 0.4%. The conductivity activation energies as presented in Table 2 and Fig. 4(a) are 0.54 eV, 0.46 eV, and 0.34 eV for the n-type a-Si:H films with $S_d = 0.1$, 0.2, and 0.4, respectively. The reduction of the conductivity activation energy indicates that the Fermi energy level (E_F) shifts towards the bottom of the conduction band (E_c) due to the doping effect. Figure 4(b) shows the energy band diagrams of the silicon thin film heterojunction solar cells with different emitter layer doping concentrations. The gap between E_c and E_F of the n-type a-Si:H layers is determined by E_a shown above. The conduction band offset ΔE_c, which is a barrier for electron transport, is formed due to the difference in electronic affinity between the epitaxial c-Si and a-Si:H,[21,23] and is a fixed value which will not be affected by the emitter layer concentration. The total diffusion potential (qV_d) across the junction, which directly affects V_{oc} of the solar cell, can be expressed as

$$qV_d = qV_d^{a-Si} + qV_d^{c-Si}, \tag{2}$$

where qV_d^{a-Si} and qV_d^{c-Si} are the diffusion potentials in a-Si:H and c-Si, respectively. We define $g = qV_d - \Delta E_c$ to describe the ability of the electrons to transfer across the junction. Under the low emitter layer doping concentration ($S_d = 0.1\%$), the conduction band E_c of n-type a-Si:H emitter layer is located at position i in Fig. 4(b). The qV_d is quite small due to the minor qV_d^{a-Si}. Thus, a lowest V_{oc} is obtained. Electrons cannot drift to the electrode sufficiently because of the low g value, and this leads to a low J_{sc}. The low doping concentration also results in a high series resistance, which may be the reason for the low FF. By increasing the emitter layer doping concentration S_d to 0.2%, E_c of the emitter layer is shown at position ii in Fig. 4(b). In this case, higher qV_d and g, and a lower series resistance are obtained. As a result, higher V_{oc}, J_{sc}, and FF are achieved. However, if the doping concentration

is further increased (E_c of the emitter layer at position iii in Fig. 4(b)), the efficiency will deteriorate although the highest V_{oc} and FF are obtained. This may be attributed to the following reason: an excessively high doping concentration further enhances the total diffusion potential qV_d and lowers the series resistance, so the highest V_{oc} and FF are obtained. Meanwhile, the high doping concentration means that more impurity atoms and defects are introduced into the emitter layer. This can greatly increase the carrier recombination velocity in the emitter layer, which leads to the lowest J_{sc}. Thus, the conversion efficiency of this solar cell is reduced compared with that of the solar cell with the emitter layer doping concentration of 0.2%.

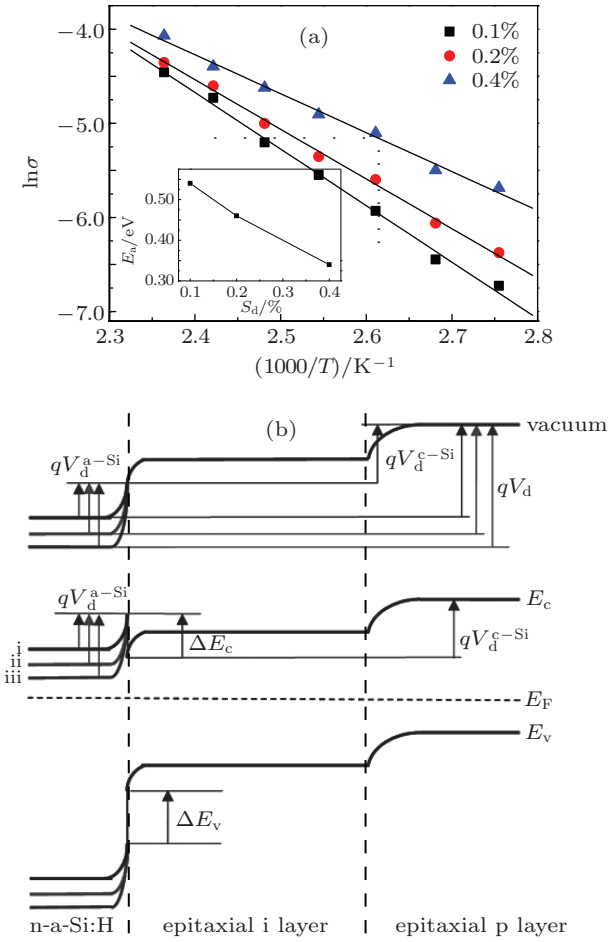


Fig. 4. (color online) (a) Temperature-dependent conductivities of the n-type a-Si:H films with different doping concentrations and the calculated activation energies of these n-type a-Si:H films (inset). (b) Schematic band diagrams of the silicon thin film heterojunction solar cells with different emitter layer doping concentrations, line i for $S_d = 0.1\%$, ii for $S_d = 0.2$, and iii for $S_d = 0.4\%$.

Figure 5 shows the curves of EQE versus wavelength of silicon thin film heterojunction solar cells with different doping concentrations of emitter layer. The results show that each of all the solar cells has a low spectral response in the blue wavelength range (300–500 nm) which results from the absorption of the front glass and glue. Of the solar cells with three different emitter layer concentrations, the solar cell with an emitter layer concentration of 0.2% exhibits the highest external quantum efficiency in a broad wavelength range from 300 nm to 1200 nm, which is in accordance with the *J*–*V* results shown in Fig. 3. It is noticeable that the EQE of the cell with $S_d = 0.4\%$ is particularly low in the wavelength range from 600 nm to 800 nm, which may be caused by the band gap narrowing effect. By introducing impurity dopants, the impurity level will be generated in the forbidden band of the semiconductor. If the impurity concentration is relatively high, the impurity atoms will be quite close to each other, which causes the wave functions of the impurity atoms to overlap and the impurity level to expand and form an impurity energy band. As a result, the band gap could become narrower than the regular band gap. From this point of view, the absorption coefficients α of the emitter layers with different doping concentrations are characterized and the band gaps are calculated from the absorption coefficients. Figure 6 shows the curves of $(\alpha h\upsilon)^{1/2}$ versus $h\upsilon$, where $h\upsilon$ is the energy of the photons. From this figure, we can see that the band gaps of a-Si:H films with $S_d = 0.1\%$ and $S_d = 0.2\%$ are almost the same, while the band gap of the film with $S_d = 0.4\%$ is reduced by about 0.05 eV. This is mainly because the excessively high doping concentration reduces the band gap by the band gap narrowing effect.

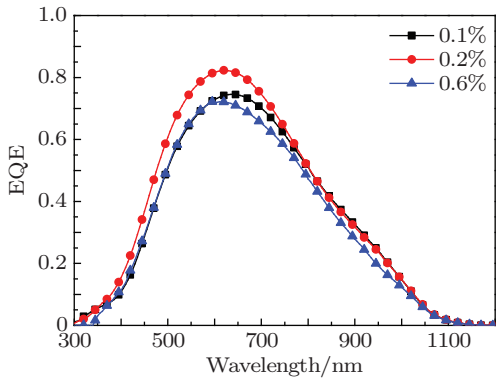


Fig. 5. (color online) External quantum efficiencies (EQE) versus wavelength of the silicon thin film heterojunction solar cells with different emitter layer doping concentrations.

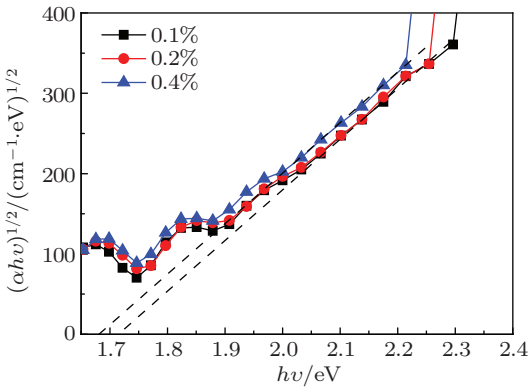


Fig. 6. (color online) The $(\alpha h\upsilon)^{1/2}$ versus $h\upsilon$ for the n-type a-Si:H films with different doping concentrations.

Thus, compared with emitter layers of lower doping concentrations ($S_d = 0.1\%$ and $S_d = 0.2\%$), the emitter layer with $S_d = 0.4\%$ would absorb more light in the wavelength range of 600–800 nm. This absorption will reduce the intensity of the light reaching the absorber layer, thereby leading to the low spectral response of the cell with $S_d = 0.4\%$.

4. Conclusion

We fabricate silicon thin film heterojunction solar cells by using a combination of the layer transfer technique and HWCVD. By increasing the emitter layer doping concentration S_d from 0.1% to 0.4%, the conductivity activation energy is reduced from 0.54 eV to 0.34 eV, which causes the solar cell conversion efficiency of the solar cell first to increase and then to decrease. A band gap reduction of 0.05 eV is observed for the n-type a-Si:H film with $S_d = 0.4\%$. The silicon thin film heterojunction solar cell with $S_d = 0.2\%$ shows the best external quantum efficiency and a maximum conversion efficiency of 7.9%.

References

[1] Han X Y, Hou G F, Zhang X D, Wei C C, Li G J, Zhang D K, Chen X L, Sun J, Zhang J J, Zhao Y and Geng X H 2009 *Chin. Phys.* B **18** 3563

[2] Zhang X D, Zheng X X, Xu S Z, Lin Q, Wei C C, Sun J, Geng X H and Zhao Y 2011 *Chin. Phys.* B **20** 108801

[3] Ni J, Zhang J J, Cao Y, Wang X B, Li C, Chen X L, Geng X H and Zhao Y 2011 *Chin. Phys.* B **20** 087309

[4] Wang G H, Zhang X D, Xu S Z, Zheng X X, Wei C C, Sun J, Xiong S Z, Geng X H and Zhao Y 2010 *Chin. Phys.* B **19** 098102

[5] Tyanaka H, Yamauchi K and Matsushita T 1998 *Proceedings of the 2nd World Conference on Photovoltaic Solar Energy Conversion*, July 6–10, 1998 Vienna, Austria, p. 156

[6] Reuter M, Brendle W, Tobail O and Werner J 2009 *Sol. Energy Mater. Sol. Cells* **93** 704

[7] Brendel R, Auer R and Artmann H 2001 *Prog. Photovoltaics* **9** 217

[8] Armigliato A, Nobili D, Solmi S, Blendin G, Schum B, Lachowicz A and Horzel J 2011 *Sol. Energy Mater. Sol. Cells* **95** 3099

[9] Xiong C, Yao R H and Geng K W 2011 *Chin. Phys.* B **20** 057302

[10] Gordon I, Vallon S, Mayolet A, Beaucarne G and Poortmans J 2010 *Sol. Energy Mater. Sol. Cells* 94 381

[11] Solanki C S, Carnel L, Van Nieuwenhuysen K, Ulyashin A, Posthuma N, Beaucarne G and Poortmans J 2005 *Prog. Photovoltaics* **13** 201

[12] Hernández-Como N, Morales-Acevedo A and Matsumoto Y 2011 *Sol. Energy Mater. Sol. Cells* 95 1996

[13] Schüttauf J, van der Werf C, van Sark W, Rath J and Schropp R 2011 *Thin Solid Films* **519** 4476

[14] Branz H, Teplin C, Young D, Page M, Iwaniczko E, Roybal L, Bauer R, Mahan A, Xu Y, Stradins P T and Wang Q 2008 *Thin Solid Films* **516** 743

[15] Stragier A, Signamarcheix T, Salvetat T, Nolot E, Dechamp J, Mercier D, Gergaud P, Tauzin A, Clavelier L and Lemiti M 2011 *J. Electrochem. Soc.* **158** H595

[16] Cai H, Shen H, Zhang L, Huang H, Lu L, Tang Z and Shen J 2010 *Physica* B: *Condens. Matter.* **405** 3852

[17] Sakata H, Nakai T, Baba T, Taguchi M, Tsuge S, Uchihashi K and Kiyama S 2000 *Conference Record of the Twenty-Eighth IEEE Photovoltaic Specialists Conference*, September 15–22, 2000 Anchorage, USA, p. 7

[18] Tanaka M, Taguchi M, Matsuyama T, Sawada T, Tsuda S, Nakano S, Hanafusa H and Kuwano Y 1992 *Jpn. J. Appl. Phys.* **31** 3518

[19] Hsiao J, Chen C, Lin C and Wu D 2011 *J. Electrochem. Soc.* **158** H876

[20] Dao V, Lee Y, Kim S, Kim Y, Lakshminarayan N and Yi J 2011 *J. Electrochem. Soc.* **158** H312

[21] Mikolasek M, Racko J, Harmatha L, Gaspierik P and Sutta P 2010 *Appl. Surf. Sci.* **256** 5662

[22] Song C, Xu J, Chen G, Sun H, Liu Y, Li W, Xu L, Ma Z and Chen K 2010 *Appl. Surf. Sci.* **257** 1337

[23] Gudovskikh A, IbrahiM S, Kleider J, Damon-Lacoste J, Cabarrocas P, Veschetti Y and Ribeyron P 2007 *Thin Solid Films* **515** 7481